3

Magnetic Carbon Nanotubes: Synthesis, Characterization and Anisotropic Electrical Properties

Il Tae Kim and Rina Tannenbaum*
Georgia Institute of Technology
United States

1. Introduction

Carbon nanotubes (CNTs) have been the focus of extensive research in recent years due to their exceptional mechanical, thermal, and electrical properties (Treacy et al., 1996; Lourie et al., 1998; Yu et al., 2000; Lukic et al., 2005). As a result of their nanoscale dimensions and high surface area, CNTs could also be considered as efficient templates for the assembly and tethering of nanoparticles on their surface (Grzelczak et al., 2006). The decoration of CNTs with various compounds and various structures could increase their surface functionality and the tunability of their properties, such as their electrical and magnetic characteristics (Korneva et al., 2005; Kuang et al., 2006). Recent reports described the attachment of various inorganic nanoparticles to either the external surface of the CNTs, or to the internal surface of the CNT cavity, through several experimental methods (Han et al., 2004; Qu et al., 2006). In this context, it is important to note that the control of the size of these tethered nanoparticles is of primary importance for the purpose of tailoring the physical and chemical properties of these hierarchical materials.

Iron oxide nanoparticles, such as magnetite and maghemite, have been of technological and scientific interest due to their unique electrical and magnetic properties. These nanoparticles can be used in such diverse fields as high-density information storage and electronic devices (Sun et al., 2000; Pu et al., 2005; Yi et al., 2006; Jia et al., 2007; Wan et al., 2007). Maghemite, γ-Fe_2O_3, is the allotropic form of magnetite, Fe_3O_4 (Rockenberger et al., 1999; Pileni et al., 2003; Sun et al., 2004). These two iron oxides are crystallographically isomorphous. The main difference is the presence of ferric ions only in γ-Fe_2O_3, and both ferrous and ferric ions in Fe_3O_4. As a result, while the magnetic properties of Fe_3O_4 are superior, γ-Fe_2O_3 is more stable, since the iron cannot be further oxidized under ambient conditions. This renders γ-Fe_2O_3 nanoparticles easier to work with, especially in the presence of organic solvents and organic ligands, and consequently, they have been widely used for magnetic storage in a variety of fields such as floppy disks and cassette tapes. However, maghemite-CNT nanohybrid materials have not been studied as extensively as magnetite-CNT nanohybrid materials, with the exception of several few examples (Sun et al., 2005; Youn et al., 2009).

*All correspondences should be addressed to rinatan@mse.gatech.edu or 404-385-1235.

The alignment of CNTs in a variety of matrices can be used to reinforce, intensify, and enhance some of the properties of the resulting systems, as well as introduce various degrees of anisotropy into the properties of the desired nanomaterials (Kimura et al., 2002; Garmestani et al., 2003). The alignment of CNTs in a suspension under a magnetic field requires that the energy produced by the torque acting on a magnetically-anisotropic segment exceeds the thermal energy of that particular segment, such that: $\delta U \sim B^2 n \delta\chi > kT$, where B is the field strength, n is the number of carbon atoms in the segment, and $\delta\chi$ is the magnetic anisotropy (Fisher et al., 2003). However, due to the low magnetic susceptibility of CNTs, their alignment by the application of an external magnetic field requires a relatively high magnetic field (Camponeschi et al., 2007). This drawback could be eliminated by enhancing the magnetic susceptibility of carbon nanotubes via the tethering of magnetic nanoparticles onto their surface. In zero field, the magnetic moments of the maghemite nanoparticles randomly point in different directions, resulting in a vanishing net magnetization. However, if a sufficient homogeneous magnetic field is applied, the magnetic moments of the nanoparticles align in parallel, and the resulting dipolar interactions are sufficiently large to overcome thermal motion and to reorient the magnetic CNTs.

In this chapter, we describe and report a convenient approach for the decoration of CNTs with near-monodisperse maghemite nanoparticles by employing a novel and simple modified sol-gel process (in-situ process) with an iron salt as precursor, followed by calcination. The resulting hybrid nanomaterials are superparamagnetic at room temperature and are conducive to facile alignment under relatively low magnetic fields. Subsquently, the nanohybrid materials, i.e. the magnetized carbon nanotubes, were incorporated into a polymer matrix and aligned by the application of a magnetic field, forming polymer composites with an aligned filler phase. It is therefore expected that the composites formed in this manner would exhibit anisotropic mechanical and electrical properties that would depend on and correlate with the parallel and perpendicular direction to the magnetic field that has been applied and under which the alignment has taken place.

2. Experimental details

2.1 Synthesis of maghemite-MWCNT nanohybrid materials

Pure-MWCNTs were first dispersed in a solution mixture of concentrated H_2SO_4 and HNO_3 with the volume ratio of 3:1. The suspension was ultra-sonicated for 3 hrs at room temperature. After that, the concentration of the suspension was diluted up to 50% and filtered with a PTFE membrane (0.45 μm pore size) with the aid of a vacuum pump. Carboxylated MWCNT (MWCNT-COOH) was washed with de-ionized water several times to reach neutral pH and dried under vacuum at 50 °C overnight. The synthesis of maghemite-MWCNT was performed by first adding 0.65 g $Fe(NO_3)_3 \cdot 9H_2O$ to 20 ml of absolute ethanol (100% purity) and stirring until the $Fe(NO_3)_3 \cdot 9H_2O$ was dissolved completely. Subsequently, this iron salt solution was added to a suspension of oxidized MWCNTs with a mass ratio of 4:1 ($Fe(NO_3)_3 \cdot 9H_2O$: MWCNTs mass ratio of 4:1), stirred, and sonicated for 3 hrs. Twenty ml of 1.2 mM of NaDDBS were added to the solution and stirred for 30 min. Then, 1.2 ml of propylene oxide was added as a gelation agent and stirred for 30 min. The mixture was then placed in a Fisher Scientific iso-temperature oven for drying for 3 days at 100 °C. The resulting powder products were washed with ethanol

several times and dried at 50 °C. The calcination of these powders was performed in a furnace under argon atmosphere at both 500 °C and 600 °C for 2 hrs. The overall strategy for the preparation of MWCNT/γ-Fe_2O_3 is shown in Figure 1 (Kim et al., 2010).

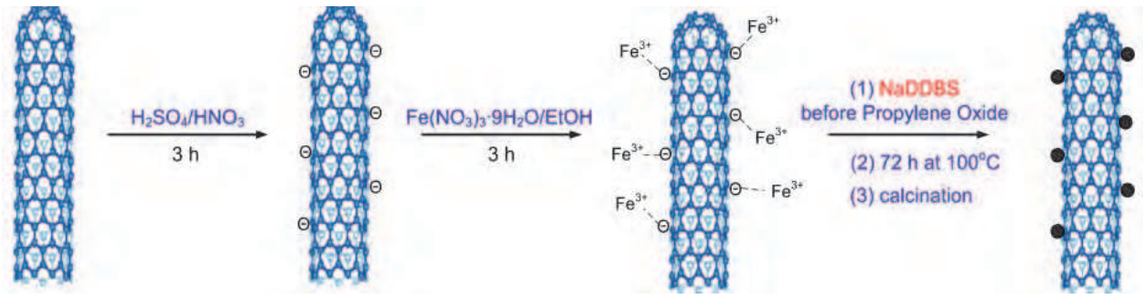

Fig. 1. Schematic representation for the preparation of nanohybrid materials, MWCNT/γ-Fe_2O_3 via a modified sol-gel technique (Reprinted with permission from Kim et al., *J. Phys. Chem. C* 2010, 114, 15, 6944-6951, Copyright 2010 ACS).

2.2 Fabrication of polymer nanocomposites with aligned feature

Various weight percents of magnetic multi-walled carbon nanotubes (m-MWCNTs) were dispersed in a small amount of ethanol with sonication for 1 hr. Epoxy resin (PR2032) was added to the suspension and mixed with a mechanical stirrer for 30 min in order to obtain optimal dispersion. After that, the nanocomposite solution was sonicated to evaporate entire solvent at 50 °C. The curing agent (PH3660) was added into the solution, mixed, and degassed under vacuum. The solution was immediately poured into a mold, and a 0.3 T magnetic field was applied for 1 hr at room temperature, for 1 hr at 60 °C, and for another 1 hr at 60 °C without a magnetic field. The nanocomposite was post-cured at 60 °C for 6 hrs in the iso-temperature oven (Kim et al., 2011).

2.3 Characterization

The dried samples were ground into a fine powder using a ceramic mortar and pestle. Tiny amounts of samples were rarified with KBr powder, ground, and pressed in a KBr pellet with a punch and die. A Nicolet Nexus 870 spectrometer scanned the range from 4000 to 400 cm^{-1} with a resolution of 2 cm^{-1} and data spacing of 0.964 cm^{-1}. XRD measurements were performed using an X'pert Pro Alpha-1 (wavelength of 1.54 Å). XRD peaks were collected from $2\theta = 0°$ to 90° with a step size of 0.02°. XPS scans of powder samples were taken using a Surface Science Laboratories SSX-100 ESCA spectrometer using monochromatic Al Kα radiation (1486.6 eV). Raman spectra were recorded in the range of 200-2000 cm^{-1} at ambient temperature using a WITEC Spectra Pro 2300I spectrometer equipped with an Ar-ion laser, which provided a laser beam of 514 nm wavelength. The magnetic properties of MWCNTs were measured using a 5.5 T Quantum Design Superconducting Quantum Interface Device (SQUID) magnetometer. The alignment of the sample was conducted by a magnet (GMW-5403) at 0.3 T. The morphology and aligned feature of as-prepared samples were also characterized using SEM (LEO 1530). TEM samples were prepared by placing a droplet of solution onto a TEM grid, and for the observation of aligned features, samples were micro-tomed into 100 nm thick slices using a diamond knife and placed on a TEM grid. These samples were analyzed using a Hitachi HF2000, 200 kV transmission electron microscopy.

The electrical conductivity data of as-prepared composites were collected using impedance analyzer (Solartron Instruments SI 1260 with dielectric interface 1296) for the frequency range 0.1 Hz ~ 1 MHz. All the data were collected under an AC voltage of 0.1 V. Contact was achieved by silver painting the two ends of the samples, and then using coaxial probers on a probe station attached to the impedance analyzer (Peng et al., 2008).

3. Decoration of carbon nanotubes with magnetic nanoparticles and the characteristics of the resulting hybrid nanostructures

A variety of methods to form nanohybrid materials on the surface of CNTs have been reported. Correa-Duarte group (Correa-Duarte et al., 2005) coated CNTs with iron oxide nanoparticles (magnetite/maghemite) via a layer by layer (LBL) assembly technique and aligned CNT chains in relatively small external magnetic fields. Subsequently, the resulting magnetic CNT structures could be used as building blocks for the fabrication of nanocomposite materials. Cai group (Wan et al., 2007) decorated CNTs with magnetite nanoparticles in liquid polyols. As a result, these nanoparticles could have significant potential for application in the fields of sensors. In addition, Gao group (Jia et al., 2007) initiated the self-assembly of magnetite particles along MWCNTs via a hydrothermal process. The resulting materials feature nanoparticle beads along the CNT surface, rendering this as an appropriate material to be used as a functional device.

The maghemite-CNT nanocomposite systems also have been reported even though research has not been studied as extensively as magnetite-CNT system. Liu group (Sun et al., 2005) decorated MWCNTs with maghemite via the pyrolysis of ferrocene at different temperatures. This product is expected to provide an efficient way for the large-scale fabrication of magnetic CNT composites. Jung group (Youn et al., 2009) decorated single-wall CNTs (SWCNTs) with iron oxide nanoparticles along the nanotube via a magneto-evaporation method. The nanotubes were aligned vertically on ITO surfaces, suggesting the possibility of rendering this process adequate and cost-effective for mass production. The method described in this work consisted of the use of an iron-oleate complex, oleic acid, and truncated SWCNTs to create iron oxide nanoparticles. The research also demonstrated the anisotropic properties of vertically aligned SWCNTs in a nanocmoposite by comparing current densities of the aligned and non-aligned CNTs.

Keeping pace with these researches' streaming, we have developed the MWCNT/γ-Fe_2O_3 nanohybrid materials. As a first step, the MWCNTs were carboxylated in order to introduce negative charges on their surface, which in turn will interact with Fe (III) ions present in a strong acid solution. This process was also coupled with sonication to ensure dispersion of the MWCNTs in the suspension. The x-ray photoelectron spectroscopy (XPS) wide-survey (Fig. 2a) and high resolution spectra (Fig. 2b) reveal not only the presence of carbon-carbon bonding of MWCNTs at 285 eV binding energy but also the formation of a carbonyl moiety consistent with carboxylated groups at 288 eV binding energy. Nucleation sites for the iron oxide were generated at the CNT surface due to the electrostatic interaction between Fe (III) ions and the carboxylate surface groups of acid-treated CNTs. In this system, the occurrence of gelation was inhibited by the addition of a surface active molecule, sodium dodecylbenzenesulfonate (NaDDBS), before the addition of propylene oxide, which is a gel promoter. The surfactant interfered in the growth stage of the iron oxide nanoparticles (gel phase) and prevented the formation of a gel. This occurred because the NaDDBS molecules had already coordinated to the iron (III) centers due to the attraction between the

negatively-charged hydrophilic head of the surfactant and the positively-charged iron (Matarredona et al., 2003; Camponeschi et al., 2008). Therefore, due to the presence of the NaDDBS molecules, no aggregates of γ-Fe_2O_3 were formed but rather the nanoparticles remained individually isolated and dispersed along the length of the CNTs.

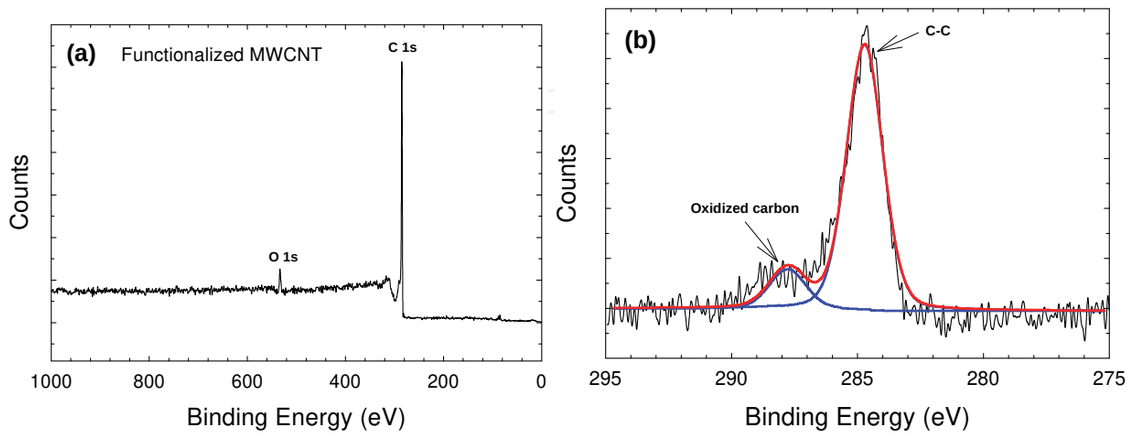

Fig. 2. (a) The XPS survey spectrum of functionalized MWCNTs. (b) The high-resolution XPS spectrum of C1s. (Adapted with permission from Kim et al., *J. Phys. Chem. C* 2010, 114, 15, 6944-6951, Copyright 2010 ACS).

X-ray diffraction patterns of MWCNT containing iron oxide nanoparticles calcinated at different temperatures with the initial $Fe(NO_3)_3 \cdot 9H_2O$: MWCNTs mass ratio of 4:1 and 2:1 demonstrate the high crystalline nature of the nanoparticles as shown in Figure 3. The diffraction peak at $2\theta = 26^\circ$ can be confidently indexed as the (002) reflection of the MWCNTs, similar to that of pure MWCNTs. The other peaks in the range of $20^\circ < 2\theta < 80^\circ$ correspond to the (220), (311), (400), (422), (511), (440), and (533) reflections of maghemite (γ-Fe_2O_3) and/or magnetite (Fe_3O_4). When the mass ratio of $Fe(NO_3)_3 \cdot 9H_2O$ and MWCNTs increases from 2:1 to 4:1, the intensity of the carbon (002) reflection decreases. Also, when calcination temperature increases from 500 °C to 600 °C, the crystal structure of the product becomes better-defined. Because XRD patterns of maghemite and magnetite are practically identical (Sun et al., 2005), x-ray diffraction alone cannot be used to distinguish between the two phases. Therefore, we employed additional experimental techniques to discern between these two phases.

The FTIR spectrum of the product of this modified sol-gel process shows the presence of well-crystallized iron oxide nanoparticles after calcination at 600 °C as shown in Figure 4. Maghemite (γ-Fe_2O_3) has an inverse spinel structure and therefore, it can be seen as an iron-deficient form of magnetite. If the powder is not heat-treated, a weak peak from 800 to 400 cm^{-1} is shown. This is evidence of an amorphous iron oxide phase with minimal long-range order typical of maghemite or magnetite. However, after calcination, IR bands show strong peaks at 576 and 460 cm^{-1}, which correspond to a partial vacancy ordering in the octahedral positions in the maghemite crystal structure (White et al., 1967; deFaria et al., 1997; Millan et al., 2007).

X-ray photoelectron spectroscopy (XPS) as well as Raman spectroscopy confirmed that the iron oxide nanoparticles formed were indeed maghemite and not magnetite. After the formation of oxidized MWCNTs decorated with iron oxide nanoparticles followed by

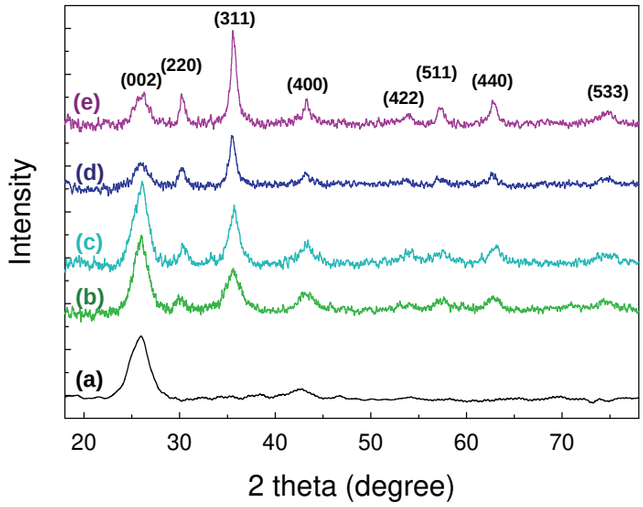

Fig. 3. XRD patterns of MWCNT/γ-Fe_2O_3 nanostructures fabricated with two different mass ratios of $Fe(NO_3)_3$ $9H_2O$ and MWCNTs: (a) MWCNT; (b) 2:1 at 500 °C; (c) 2:1 at 600 °C; (d) 4:1 at 500 °C; (e) 4:1 at 600 °C (Reprinted with permission from Kim et al., *J. Phys. Chem. C* 2010, 114, 15, 6944-6951, Copyright 2010 ACS).

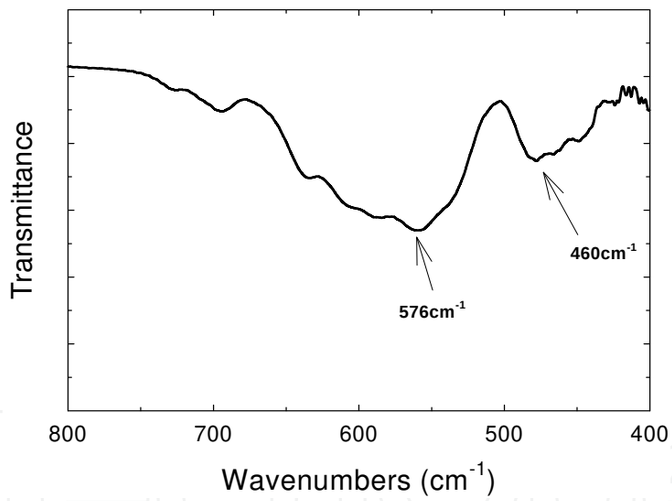

Fig. 4. FTIR spectrum of MWCNT/γ-Fe_2O_3 after calcination at 600 °C (Reprinted with permission from Kim et al., *J. Phys. Chem. C* 2010, 114, 15, 6944-6951, Copyright 2010 ACS).

calcination at 600 °C, Figure 5 shows XPS characteristic iron peaks in addition to carbon and oxygen. The position of the Fe (2p3/2) and Fe (2p1/2) peaks were marked at 711.3 and 724.4 eV, respectively, which are in good agreement with the values reported for γ-Fe_2O_3 in the literature (Hyeon et al., 2001; Sun et al., 2005). Therefore, this suggests the formation of γ-Fe_2O_3 in our samples. Raman spectroscopy can also effectively distinguish between maghemite and magnetite nanoparticles. The strong peak at ~1350 cm^{-1} can be assigned to the D band of MWCNTs, while another dominant peak at ~1576 cm^{-1} can be ascribed the G band of MWCNTs as shown in Figure 6 (Jorio et al., 2003). In contrast to magnetite, the maghemite bands are not well-defined, but rather consist of several broad peaks around

350, 500, and 700 cm^{-1}, which are unique to these species and are absent in other types of iron oxide nanoparticles (deFaria et al., 1997). This supports the conclusion that the nanoparticles bound at the walls of the MWCNTs are maghemite and not magnetite.

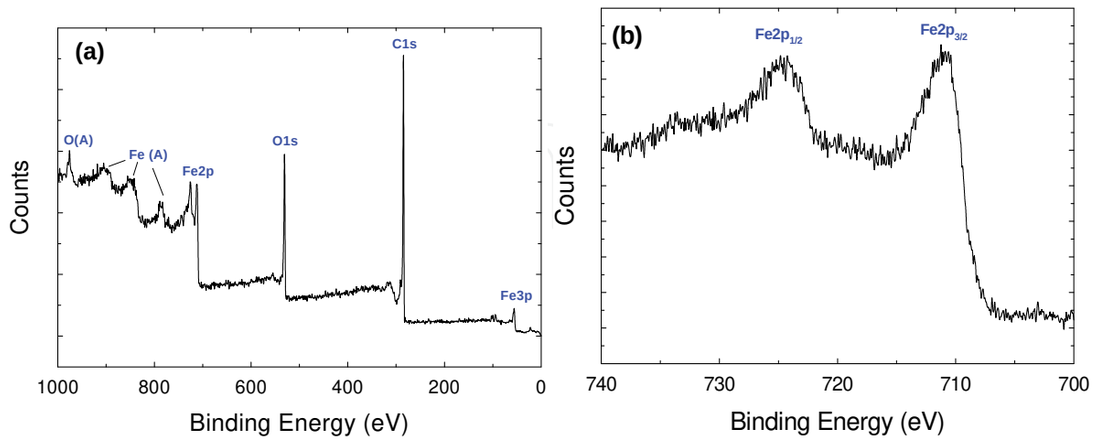

Fig. 5. (a) The XPS survey spectrum of MWCNT/γ-Fe_2O_3. (b) The high-resolution XPS spectrum of Fe 2p bands (Adapted with permission from Kim et al., *J. Phys. Chem. C* 2010, 114, 15, 6944-6951, Copyright 2010 ACS).

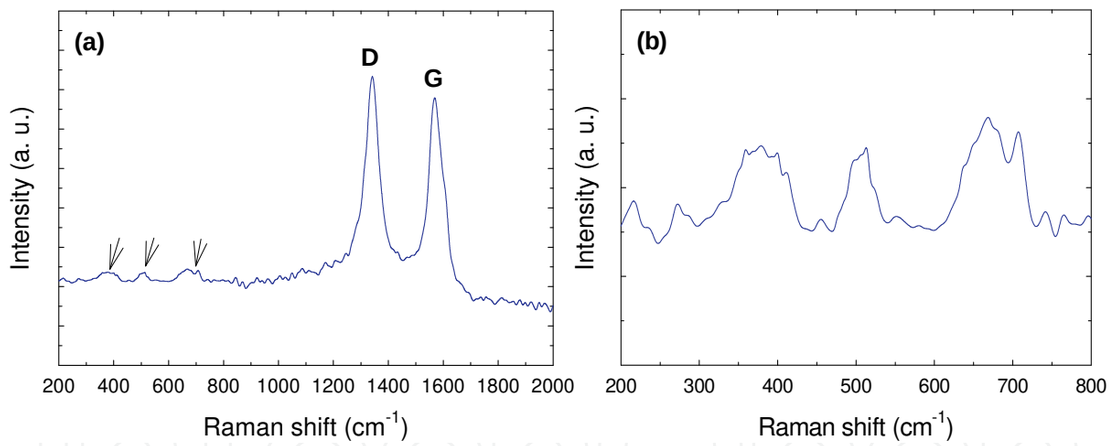

Fig. 6. (a) The Raman spectrum of MWCNT/γ-Fe_2O_3 nanostructure prepared at 600 °C with the mass ratio of 4:1. (b) The detailed Raman spectrum of the same sample in the 200-800 cm^{-1} spectral range (Reprinted with permission from Kim et al., *J. Phys. Chem. C* 2010, 114, 15, 6944-6951, Copyright 2010 ACS).

Scanning electron microscopy (SEM) and transmission electron microscopy (TEM) images of MWCNTs/γ-Fe_2O_3 confirmed that γ-Fe_2O_3 was attached to the walls of the MWCNTs as shown in Figure 7. The high-resolution transmission electron microscopy (HRTEM) image of a nanoparticle (Figure 7(b)) illustrates the maghemite interlayer spacing of the (311) lattice plane of approximately 0.25 nm (Hyeon et al., 2001). Furthermore, the inset image of Figure 7(b) shows the electron diffraction patterns of maghemite, indicating the high crystallinity of the maghemite nanoparticles. At a mass ratio of 4:1 between the $Fe(NO_3)_3 \cdot 9H_2O$ precursor and the MWCNTs, the particle size increased with increasing temperature from 500 °C to

600 °C, and the average sizes were 10.1 nm and 10.8 nm, respectively as shown in Figure 7(c) and (d). Similarly, when the mass ratio of $Fe(NO_3)_3 \cdot 9H_2O$ precursor and MWCNT was 2:1, the average particle sizes as a result of the increased temperature were 7.9 nm and 8.4 nm, respectively (Figure 7(e) and 7(f)), which also slightly increased with increasing temperature. This result indicated that both a higher mass ratio between the $Fe(NO_3)_3 \cdot 9H_2O$

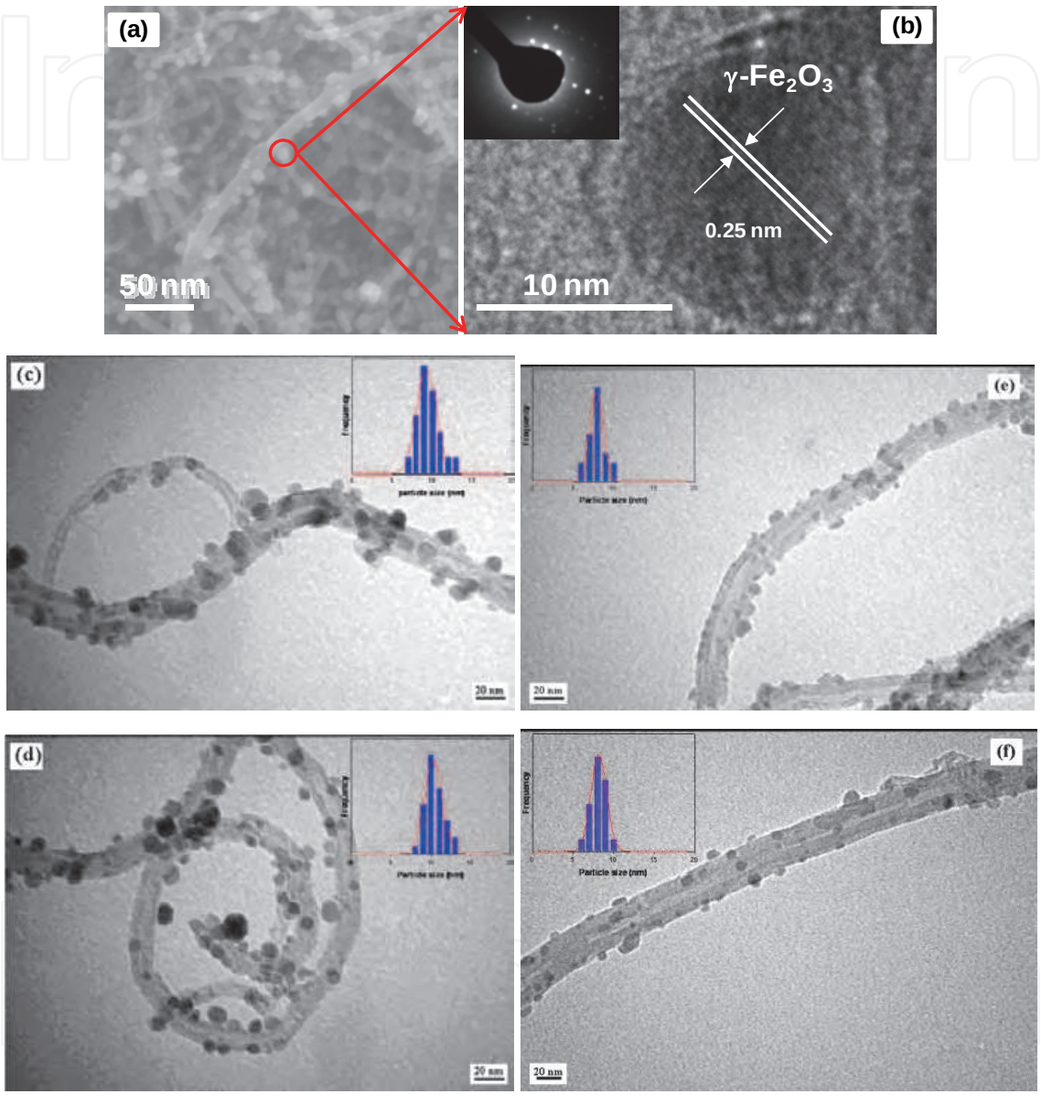

Fig. 7. (a) SEM image of MWCNT/γ-Fe_2O_3 hybrid structures prepared with 4:1 mass ratio of iron salt and MWCNT; (b) High resolution TEM image of maghemite. Inset shows diffractions of a single maghemite nanoparticle. TEM images of MWCNT/γ-Fe_2O_3 prepared with 4:1 mass ratio of iron salt and MWCNT: (c) High-resolution image prepared at 500 °C; (d) High magnification image prepared at 600 °C. TEM images of MWCNT/γ-Fe_2O_3 prepared with 2:1 mass ratio; (e) High magnification image prepared at 500 °C; (f) High magnification image prepared at 600 °C (Adapted with permission from Kim et al., *J. Phys. Chem. C* 2010, 114, 15, 6944-6951, Copyright 2010 ACS, and Kim et al., *Carbon* 2011, 49, 1, 54-61, Copyright 2011 Elsevier).

precursor and the MWCNT and increasing temperature led to larger nanoparticles, and therefore, we can conclude that particle size could be controlled by the precursor to MWCNT mass ratio and temperature.

Chemical analysis using EDS during the TEM analysis showed the presence of Fe, O, and C in the maghemite-MWCNT system as shown in Figure 8, and the calculated atomic ratio of Fe and O was close to 2:3, which suggested the formation of γ-Fe_2O_3.

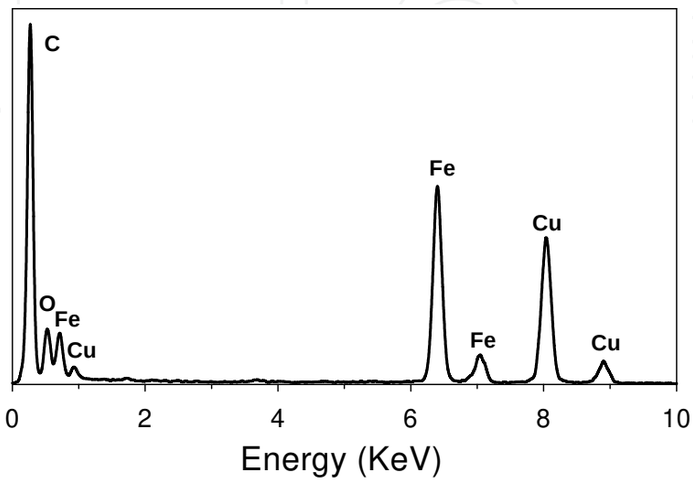

Fig. 8. Energy dispersion spectrum (EDS) of the MWCNT/γ-Fe_2O_3 hybrid material (Adapted with permission from Kim et al., *J. Phys. Chem. C* 2010, 114, 15, 6944-6951, Copyright 2010 ACS).

The magnetic properties of the as-prepared MWCNTs/γ-Fe_2O_3 nanocomposites were measured using Superconducting Quantum Interference Device (SQUID) magnetometer. The magnetization hysteresis loops were measured in fields between ±50 kOe at room temperature as shown in Figure 9(a). The saturation magnetization (M_s) of the samples obtained is below 2 emu/g, which is considerably smaller than that of bulk iron (M_s = 222 emu/g) as shown in Table 1. Coercivity is below 10 Oe, which is larger than that of bulk iron (H_c = 1 Oe). The conclusion drawn from the measurement of magnetic properties is that both samples, having different ratios between $Fe(NO_3)_3 \cdot 9H_2O$ precursor and MWCNT, exhibit superparamagnetic behavior at room temperature. This should be mainly attributed to the small size of γ-Fe_2O_3 nanoparticles that were formed in the presence of MWCNTs (Pascal et al., 1999). This result is in good accordance with the TEM observation of the small sizes of the maghemite nanoparticles mentioned above.

The magnetic attraction of our sample was also tested by placing a magnet near a vial containing the maghemite-MWCNT nanostructures as shown in Figure 9(c) and 9(d). Our samples can be easily dispersed in solution and form a stable suspension. When a magnet approaches the vial, magnetic carbon nanotubes are attracted toward the magnet. This phenomenon illustrates that the maghemite nanoparticles that are anchored on the surface of the MWCNTs impart to the composite material a magnetic response similar to that observed with magnetite.

This novel method for the magnetization of carbon nanotubes through the tethering of magnetic iron oxide nanoparticles with controlled size and site distribution would open up

a slew of new opportunities for applications in which the alignment of CNTs is not only desired, but is actually required. While many groups have studied strategies to align MWCNT/Fe_3O_4 nanostructures under external magnetic fields due to their strong magnetic properties, very little attention has been devoted to MWCNT/γ-Fe_2O_3 conjugate nanomaterials. Therefore, we would like to show that this latter system also exhibits similar interesting properties and can constitute a facile gateway to MWCNT alignment processes under tight morphological control and relatively low magnetic fields, resulting in enhanced anisotropic electrical conductivity behavior, in the following sections.

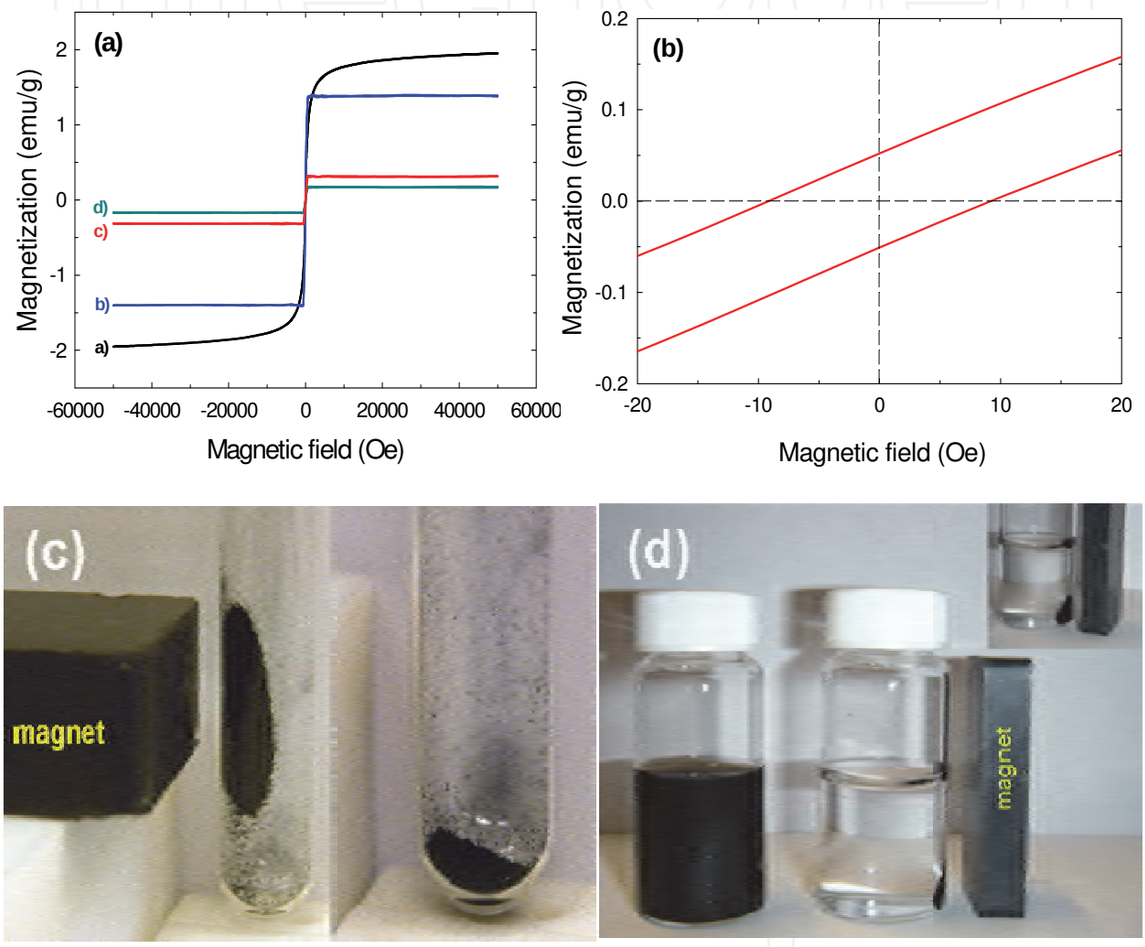

Fig. 9. (a) Magnetization vs. applied magnetic field for the magnetic carbon nanotubes prepared at different mass ratios and temperatures: 4:1 mass ratio of $Fe(NO_3)_3 \cdot 9H_2O$ and MWCNT at a) 500 °C, b) 600 °C, and 2:1 mass ratio of $Fe(NO_3)_3 \cdot 9H_2O$ and MWCNT at c) 500 °C, d) 600 °C. (b) The enlarged hysteresis loop of the MWCNT/γ-Fe_2O_3 structures formed from a 4:1 mass ratio of $Fe(NO_3)_3 \cdot 9H_2O$ and MWCNT calcinated at 600 °C. The photographs of magnetic carbon nanotubes (c) in the presence (left image) and in the absence (right image) of a magnet and (d) suspended in ethanol in the absence (left image) and in the presence (right image) of an externally-placed magnet (Adapted with permission from Kim et al., *J. Phys. Chem. C* 2010, 114, 15, 6944-6951, Copyright 2010 ACS, and Kim et al., *Carbon* 2011, 49, 1, 54-61, Copyright 2011 Elsevier).

Magnetic properties	Calcination temperature (°C)	2:1	4:1
M_s (emu/g)	500	0.3	2.0
	600	0.2	1.4
H_c (Oe)	500	4.8	2.8
	600	6.3	9.6

Table 1. Magnetic properties as a function of both different mass ratio of $Fe(NO_3)_3 \cdot 9H_2O$ and MWCNT and different calcination temperatures.

4. Alignment strategies of carbon nanotubes in polymer matrices

Alignments of CNTs by electric, shear induced field, and magnetic field were reported previously by several groups (Chen et al., 2001; Nagahara et al., 2002). Bauhofer group (Martin et al., 2005) successfully demonstrated the application of AC electric fields allowing both the alignment of carbon nanofibers in epoxy resin and their connection into a network. Zhu group (Zhu et al., 2009) studied electric field aligned MWCNT/epoxy nanocomposites with a sample size of up to several centimetres using fast UV polymerization, showing significant anisotropic properties for storage modulus and electrical conductivity.

For the characterization of aligned composite systems using shear induced field, we probed the effects of shear flow on the alignment of dispersed SWCNTs in polymer solutions as a previous study (Camponeschi et al., 2006). The sample solutions were placed in the 8.5 mm gap between the outer cylinder and the spindle, as shown Figure 10. In turn, the spindle was allowed to rotate for one week at several different angular velocities ranging from 12 to 100 rpm. TEM samples were taken in situ from the solutions flowing in circular motion in the gap between the outer cylinder and inner cylinder as shown in Figure 10(b).

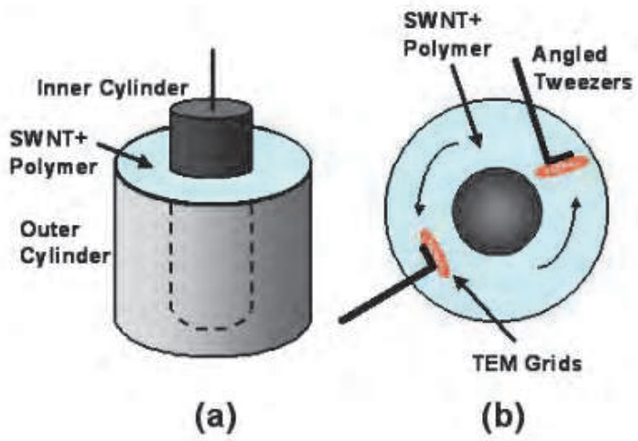

Fig. 10. (a) Concentric cylinder arrangement in the Brookfield viscometer. (b) TEM sample retrieval and preparation (Reprinted with permission from Camponeschi et al., *Langmuir* 2006, 22, 4, 1858-1862. Copyright 2006 ACS).

In this experimental set up, for systems in which effective dispersion of the carbon nanotubes was achieved by the combined action of both NaDDBS and Carboxymethylcellulose (CMC). The only system in which tube alignment was observed was for the NaDDBS/CMC/SWCNT solution that was subjected to shear stresses at the highest angular velocity used in the experiments as shown in Figure 11.

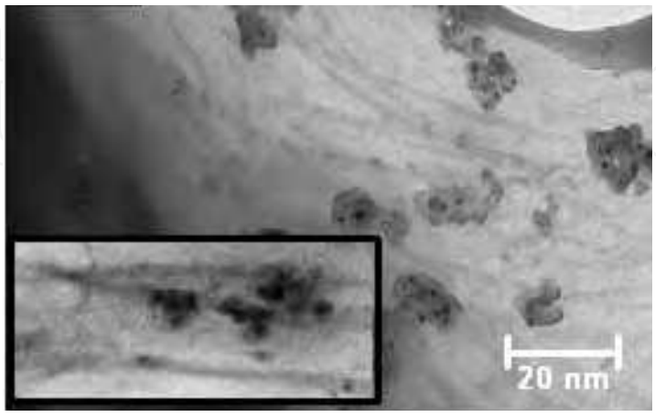

Fig. 11. Oriented carbon nanotubes dispersed with NaDDBS and CMC and subjected to shear flow at 100 rpm. The inset image is a 4-fold magnification of the larger image showing the local orientation of the surface modified SWCNT (Reprinted with permission from Camponeschi et al., *Langmuir* 2006, 22, 4, 1858-1862. Copyright 2006 ACS).

A high magnetic field is an efficient and direct ways to align carbon nanotubes. Tanimoto group have found that a high magnetic field of 7 T aligns arc-grown MWCNTs (Fujiwara et al., 2001). They dried a MWCNT dispersion in methanol under a constant magnetic field and observed the MWCNTs alignment parallel to the field. This result was explained by the difference between the diamagnetic susceptibilities parallel ($\chi_{//}$) and perpendicular ($\chi_{\perp}$) to the tube axis; if $|\chi_{\perp}|$ is larger than $|\chi_{//}|$, a MWCNT tends to align parallel to the magnetic field by overcoming thermal energy (Ajiki et al., 1993; Fujiwara et al., 2001). More recently, Steinert and Dean (Steinert & Dean, 2009) obtained solution cast PET-carbon nanotube composite films by applying a magnetic field, resulting in increased conductivity with the increase of the applied magnetic field. Furthermore, in our previous study (Camponeschi et al., 2007), we prepared magnetically aligned carbon nanotube composite systems; thus, carbon nanotubes were aligned parallel to the direction of magnetic field, resulting in enhanced mechanical properties. However, due to the low magnetic susceptibility of carbon nanotubes, their alignment by the application of an external magnetic field requires a relatively high magnetic field. This draw-back could be solved by enhancing the magnetic susceptibility of carbon nanotubes by tethering magnetic nanoparticles on their surface, as we developed MWCNT/γ-Fe_2O_3 hybrid materials.

The samples for SEM were prepared by dispersing as-prepared nanostructures in water solution with surfactant, sonicating for 30 min, and then depositing the samples onto silicon wafer under an external field. Figure 12 shows the SEM images of magnetic carbon nanotubes. When a droplet of dispersed hybrid materials in a water solution was dried under the magnetic field, the surface-modified MWCNT were aligned easily as shown in

Figure 12(a). However, when the nanocomposite solution was dried without applying magnetic field, the surface-modified MWCNT did not exhibit alignment features.

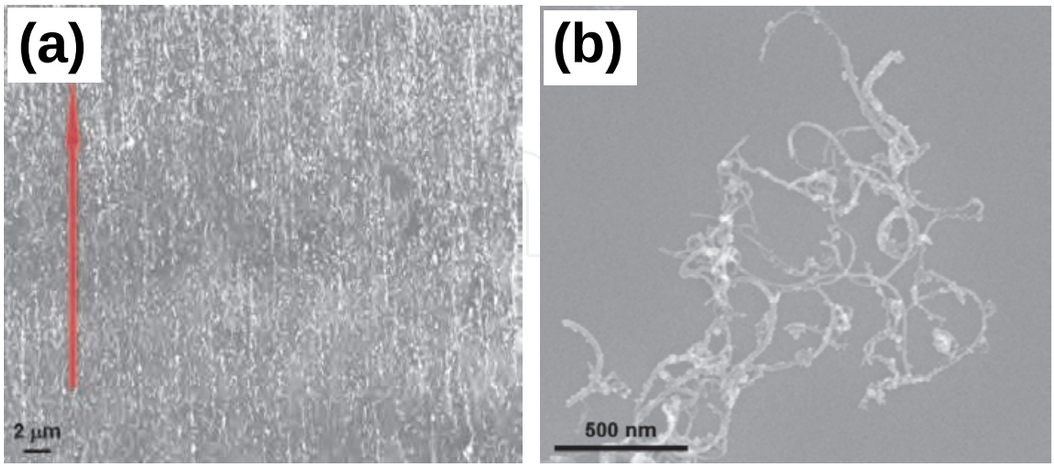

Fig. 12. (a) SEM image of aligned magnetic carbon nanotube hybrid materials parallel to the direction of magnetic field. (b) SEM image of magnetic carbon nanotube hybrid materials that were not subjected to a magnetic field (Reprinted with permission from Kim et al., *Carbon* 2011, 49, 1, 54-61.2011. Copyright 2011 Elsevier).

The TEM images of composites in which surface-modified MWCNT (m-MWCNT) and unmodified MWCNT were embedded in epoxy matrices are shown in Figure 13(a) through 13(d). We first compared the alignment features of the MWCNT/epoxy nanocomposite and the m-MWCNT/epoxy nanocomposite systems, under the same experimental conditions, i.e. the same strength of the externally-applied magnetic field (0.3 T). Figure 13(a) and 13(b), representing MWCNT/epoxy composites with 0.5 wt% MWCNT and 1.0 wt% MWCNT, respectively, did not reveal any alignment features of filler phase in the polymer matrix under the externally-applied magnetic field. However, in the case of the m-MWCNT/epoxy nanocomposite systems also having 0.5 wt% m-MWCNT and 1.0 wt% m-MWCNT and shown in Figure 13(c) and 13(d), respectively, it is obvious that the m-MWCNTs embedded in the epoxy matrix have indeed aligned parallel to the direction of magnetic field (0.3 T). Comparing the alignment features of aligned m-MWCNT hybrid materials and aligned m-MWCNT/epoxy composites (Figure 12(a), 13(c), and 13(d)), it becomes evident that the m-MWCNT hybrid materials in the absence of a polymer matrix show better alignment, fact which could be attributed to the viscosity of the polymer matrix during processing. Therefore, we can conclude that the m-MWCNT hybrids can be aligned under a relatively weak magnetic field even when embedded in a polymer matrix. This alignment is expected to directly affect the anisotropic conductivity of the resulting epoxy composites, as will be shown in the subsequent section (Figure 14 and 15). The bundling of the m-MWCNTs in the polymer matrix, as observed in the inset in Figure 13(c), may be attributed to the anisotropic nature of the dipolar interactions of the iron oxide nanoparticles near the ends of the carbon nanotubes, i.e. the near-linear stacking of the north and south poles of the m-MWCNT in the polymer matrix, resulting in their observed end-to-top connectivity (Butter et al., 2003; Correa-Duarte et al., 2005).

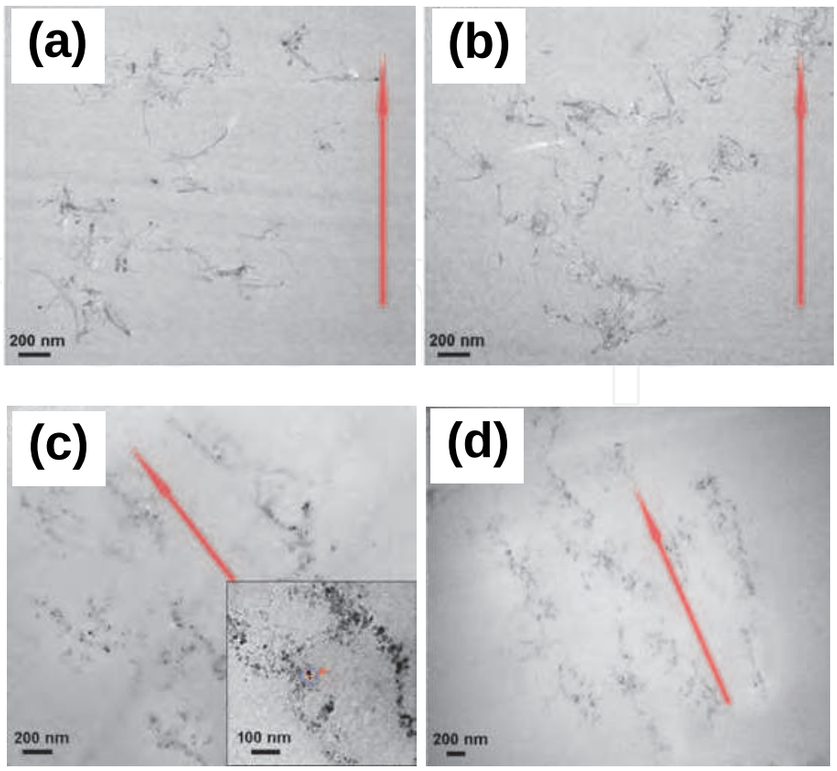

Fig. 13. (a) TEM image of MWCNT/epoxy composites with 0.5 wt% filler loading. (b) TEM image of MWCNT/epoxy composites with 1.0 wt% filler loading. (c) TEM images of m-MWCNT/epoxy composites with 0.5 wt% filler loading. Inset shows the end-to-top connectivity between two m-MWCNTs under an external magnetic field. (d) TEM image of m-MWCNT/epoxy composites with 1.0 wt% filler loading (Adapted with permission from Kim et al., *Carbon* 2011, 49, 1, 54-61. Copyright 2011 Elsevier).

5. Anisotropic electrical conductivity of composite system

The electric conductivities of the m-MWCNT/epoxy composites were measured at a series of different frequencies, from 0.1 Hz to 1 MHz. The real and imaginary parts of the impedance (Z′ and Z′′) were collected, and the magnitude of the AC conductivity (σ) was calculated using equations:

$$Z = Z' + iZ''$$

$$\sigma = \frac{1}{\sqrt{Z'^2 + Z''^2}} \frac{L}{A}$$

where, i is the imaginary unit, L is the path length along the measurement direction, and A is the electrode cross-sectional area. Figure 14 shows various conductivities of a series of m-MWCNT/epoxy nanocomposite samples containing various degrees of content of m-MWCNT in the polymer matrix. At the same magnetic field (0.3 T), the conductivity increased with increasing m-MWCNT content in composites. In the case of 0.1 wt% filler content, the nanocomposite exhibited dielectric behavior because the low mass-fraction of

m-MWCNT made it difficult to form interconnected m-MWCNT networks that would have facilitated electron flow. However, for m-MWCNT contents of 0.5 wt% and higher, the samples exhibited increased conductivity as a function of increased mass-fraction of the m-MWCNT.

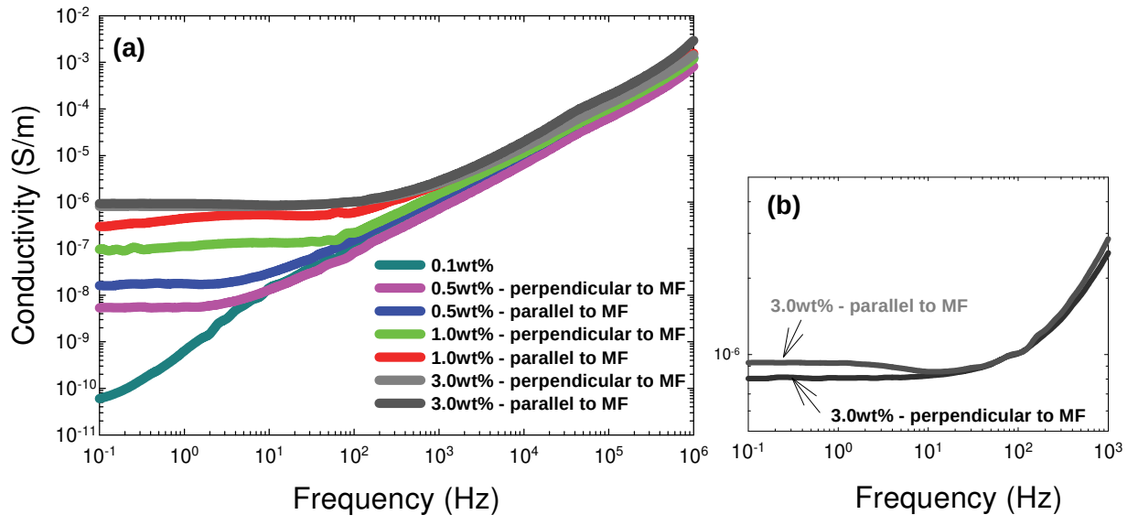

Fig. 14. (a) The conductivity of m-MWCNT/epoxy composites as a function of frequency for different mass loading of m-MWCNT as measured in the direction parallel to the magnetic field and perpendicular to the magnetic field. (b) The magnified region of a nanocomposite with a 3.0 wt% filler loading (Adapted with permission from Kim et al., *Carbon* 2011, 49, 1, 54-61. Copyright 2011 Elsevier).

Percolation theory predicts a critical concentration or percolation threshold where the material converts from a capacitor to a conductor (Weber et al., 1997; Ounaies et al., 2003). In order to determine the percolation threshold of the aligned system, the volume conductivity data could be fitted to a power law in terms of volume fraction of m-MWCNT.

$$\sigma_c \propto (v - v_c)^t$$

where σ_c is the composite conductivity, v is the m-MWCNT volume fraction in the composite, v_c is the critical volume fraction, and t is the critical exponent. We assumed that the density of m-MWCNT is the same as that of unmodified-MWCNT (2.1 g/cm^3), since both mass and volume of m-MWCNT increase similarly. The inset in Figure 15 shows the plot of σ_c as a function of $v - v_c$ for the parallel measurements. The linear fit to the data generated a straight line with v_c = 0.2 vol% (corresponding to 0.4 wt%), which gives a good fit.

When we compared the results of samples in which conductivity was measured in the direction of the m-MWCNT alignment (parallel to the magnetic field) and perpendicular to the m-MWCNT alignment (perpendicular direction to the magnetic field) for the same mass fraction of m-MWCNT, we observed that the conductivity measured parallel to the magnetic field was higher than that measured perpendicular to the magnetic field, indicating a cooperative effect due to the alignment of the m-MWCNTs in the polymer

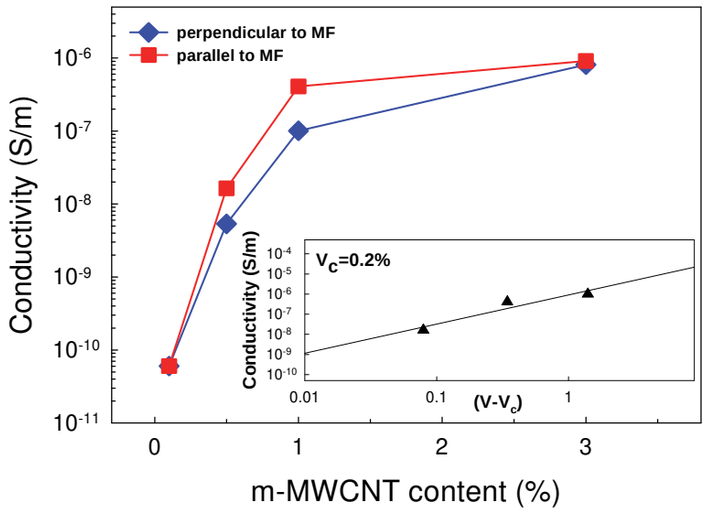

Fig. 15. The conductivity of m-MWCNT/epoxy composites as a function of different mass loading of m-MWCNT measured in the direction parallel to the magnetic field and perpendicular to it. Inset shows percolation equation fit to the experimental conductivity data obtained parallel to the direction of the magnetic field (Adapted with permission from Kim et al., *Carbon* 2011, 49, 1, 54-61. Copyright 2011 Elsevier).

matrix, as was previously shown in Figure 13(c) and 13(d). Figure 15 shows the variation of the conductivities extracted from the plateau region at low frequency as a function of m-MWCNT mass fractions in the epoxy nanocomposite for both the parallel and perpendicular directions with respect to the magnetic field. The measured conductivities are summarized in Table 2.

We would like to note that for 3.0 wt% m-MWCNT sample, even though the conductivity in the parallel direction was somewhat larger than that in the perpendicular direction (see Figure 14(b)), the values obtained were, nevertheless, quite similar. This is most likely due to the following factors: (a) We assumes that the viscosity of the composite solution containing 3.0 wt% m-MWCNT is higher than for other compositions as evidenced by the superior alignment of m-MWCNT without polymer matrix to that of m-MWCNT/epoxy composites,

m-MWCNT content (wt%)	Conductivity (S/m)		Conductivity ratio of parallel and perpendicular
	Parallel to MF	Perpendicular to MF	
3.0	1.0×10^{-6}	8.5×10^{-7}	1.2
1.0	4.1×10^{-7}	1.0×10^{-7}	4.1
0.5	1.6×10^{-8}	5.3×10^{-9}	3.0
0.1	6.0×10^{-11}		1.0

Table 2. The conductivity of m-MWCNT/epoxy composites in the directions that were parallel and perpendicular to the externally-applied magnetic field as a function of m-MWCNT content.

as discussed in a previous section. By introducing higher mass fractions of the carbon nanotubes into the polymer solution, the viscosity of the system could be further increased,

fact which could then handicap with the alignment process. Therefore, we can conclude that when the magnetic field was applied to the 3.0 wt% m-MWCNT sample, the alignment of the decorated carbon nanotubes was not as effective as in the less concentrated samples, and hence, the differences between the conductivities in the parallel and the perpendicular directions were not as pronounced, mainly due to the higher viscosity of the solution. (b) In addition, the conductivity of 3.0 wt% m-MWCNT sample (measured in either direction) was not much higher than the conductivity of the 1.0 wt% m-MWCNT sample (see Figure 15). Tethered iron oxide (maghemite) nanoparticle has high resistivity (Mei et al., 1987). Hence, the higher viscosity of the 3.0 wt% m-MWCNT sample may lead to the formation of iron oxide rich regions, resulting in a decrease of the conductivity.

6. Anisotropic response m-CNT-epoxy composite system to compression

The initial goal of using a magnetic field on carbon nanotube composites was to promote the alignment of the carbon nanotubes, which would improve the mechanical properties of the composite, particularly in the direction of the alignment. The effects on the glass transition temperature should be relatively simple to predict since they are well documented (Akima et al., 2006; Bliznyuk et al., 2006; Dou et al., 2006; Lanticse et al., 2006; Park et al., 2006). It is expected that increasing the extent of alignment and orientation of the carbon nanotubes and epoxy matrix chains (Al-Haik et al., 2004) will result in an increase in the glass transition temperature of the composite (Ajayan et al., 1994; Akima et al., 2006; Bliznyuk et al., 2006; Dou et al., 2006; Lanticse et al., 2006; Park et al., 2006). Table 3 summarizes the T_g values for the various samples tested.

Fe:CNT	Magnetic field (Tesla)	$T_g \pm 5.2$ (°C)
0:0	0	54.9
0:0	0.4	63.8
0:0	0.8	68.7
2:1	0	41.6
2:1	0.4	65.6
2:1	0.8	75.1
4:1	0	45.5
4:1	0.4	68.9
4:1	0.8	86.0

Table 3. The glass transition temperature of the m-CNT/epoxy nanocomposites measured in samples subjected to various external magnetic fields.

The glass transition temperature of the epoxy matrix increased with increasing magnetic field and implies that there is some molecular orientation/alignment occurring in the epoxy (Garmestani et al., 2003). When the magnetic CNTs are introduced into the matrix, the glass transition temperature of the nanocomposite decreased, probably due to the plasticizing effect of the NaDDBS molecules associated with the Fe_2O_3 nanoparticles tethered to the surface of the CNTs. However, in the samples in which the magnetic CNTs were aligned when the nanocomposite was subjected to an external magnetic field, the general trend showed that an increase in the extent of alignment caused an increase in T_g, as expected.

Preliminary compression data that illustrate the effect of a magnetic field on the modulus of the epoxy matrix naocomposites are shown in Figure 16.

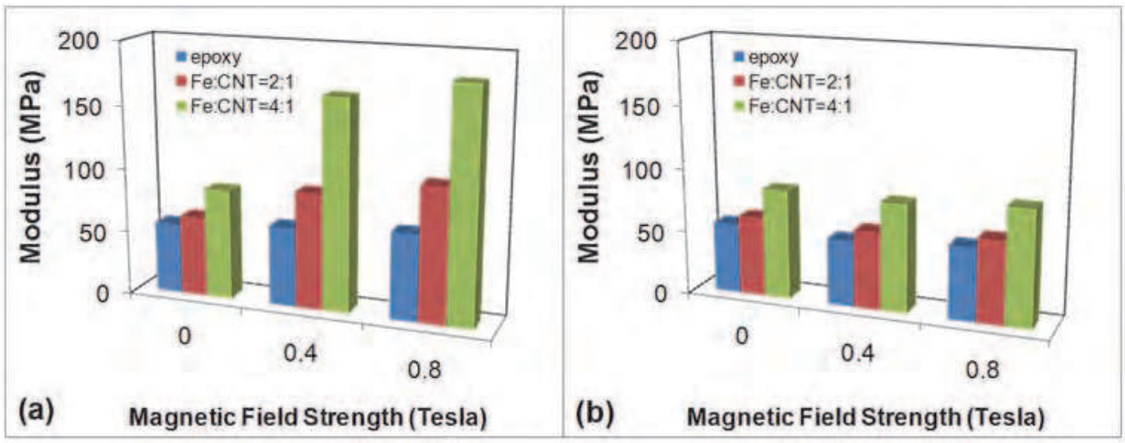

Fig. 16. The moduli of the m-CNT/epoxy nanocomposites that were subjected to an external magnetic field measured at room temperature. (a) Measured in the direction that is parallel to the applied magnetic field; (b) Measured in the direction that is perpendicular to the applied magnetic field .

The modulus was measured at room temperature both in the direction that is parallel to the applied magnetic field (Figure 16a) and in the direction that is perpendicular to the applied magnetic field (Figures 16b). The presence of the externally-applied magnetic field had little effect on the pure epoxy. It has been shown in previous work that the orientation and possible alignment of epoxy chains is indeed possible, but only at very high magnetid fields (Garmestani et al., 2003). Hence, the moduli of pure epoxy are constant, irrespective of the magnitude of the magnetic field applied on the samples and of the direction of the measurement. Conversely, the moduli observed for the epoxy filled with the m-CNTs indeed increase with the increase in the magnetic field, mainly for measurements conducted parallel to the direction of the magnetic field. Moreover, higher concentrations of the iron oxide nanoparticles tethered to the surface of the CNTs result in considerably higher moduli, particularliy in the direction parallel to the magnetic field, probably due to an increase in the susceptibility of the m-CNTs to the applied magnetic field.

7. Summary and outlook

In this chapter, we have demonstrated on CNT-inorganic hybrid system, especially, CNT/γ-Fe_2O_3 hybrid materials. We developed the synthesis method of MWCNT/γ-Fe_2O_3 nanostructures via an easy and novel modified sol-gel process. Our study shows that NaDDBS molecules are intimately involved in inhibiting the formation of an iron oxide gel. As a result, well-defined and well-dispersed maghemite nanoparticles can be obtained. In addition, the particle size of these nanoparticles could be precisely modulated by changing the temperature and the mass ratio of the $Fe(NO_3)_3$ $9H_2O$ precursor and MWCNTs. Finally, tethered γ-Fe_2O_3 magnetic nanoparticles on the surface of MWCNTs imparted superparamagnetic properties to the composite material.

Due to the acquired magnetic property of the m-MWCNTs, they could be aligned either alone or embedded in a polymer matrix by the application of only a relatively weak

magnetic field. Conductivity measurements performed on m-MWCNT/epoxy composites showed that the conductivity of the m-MWCNT/epoxy composites increased with increasing m-MWCNT contents with low percolation threshold (~0.4–0.5 wt% m-MWCNT loading). Moreover, the conductivity measured in the direction parallel to the magnetic field was higher than that measured in the direction perpendicular to it. However, the alignment of a nanocomposite sample having a loading of 3.0 wt% m-MWCNT was not as effective as samples with lower nanofiller content because of the higher solution viscosity in the more concentrated samples. This hurdle could, in principle, be overcome by either applying a stronger magnetic field or selecting other polymer matrices with low solution viscosity.
In summary, our facile magnetic functionalization method could be effectively applied for the development of conductive films, composites with conductive polymers, and bio-based composites with aligned features. Furthermore, we suggest that this maghemite-CNT hybrid material may be used for biomedical applications such as drug delivery or special medical applications such as cancer diagnosis in the not-so-distant future (Sincai et al., 2001; Sousa et al., 2001).

8. Acknowledgement

This work was supported in part by grants from NSF, Division of Engineering, award No. ECCS-0535382 and by the Air Force/Bolling AFB/DC MURI, award No. F49620-02-1-0382. Il Tae Kim was supported by a Paper Science and Engineering (PSE) Graduate Fellowships from the Institute of Paper Science and Technology (IPST) at the Georgia Institute of Technology. The authors are indebted to Drs. Erin Camponeschi, Hamid Garmestani, Karl Jacob and Allen Tannenbaum for their invaluable contributions and stimulating input.

9. References

Ajayan, P. M.; Stephan, O.; Colliex, C. & Trauth, D. (1994). Aligned carbon nanotube by cutting a polymer resin-nanotube composite. *Science*, 265, pp.1212.

Akima, N.; Iwasa, Y.; Brown, S.; Barbour, A. M.; Cao, J.; Musfeldt, J. L.; Matsui, H.; Toyota, N.; Shiraishi, M.; Shimoda, H. & Zhou, O (2006). Strong anisotropy in the far-infrared absorption spectra of stretch-aligned single-walled carbon nanotubes. *Adv. Mater.*, 18, 9, pp. 1166-1169.

Ajiki, H. & Ando, T. (1993). Magenetic-properties of carbon nanotubes, *J. Phys. Soc. Jpn.*, 62, 7, pp. 2470-2480.

Al-Haik, M. S.; Garmestani, H.; Li, D. S.; Hussaini, M. Y.; Sablin, S. S.; Tannenbaum, R. & Dahmen, K (2004). Mechanical properties of magnetically oriented epoxy. *J. Polym. Sci. Polym. Phys.*, 42, pp. 1586-1600.

Bliznyuk, V. N.; Singamaneni, S.; Sanford, R. L. Chiappetta, D.; Crooker, B. & Shibaev, P. V. (2006). Matrix mediated alignment of single wall carbon nanotubes in polymer composite films. *Polymer*, 47, 11, pp. 3915-3921.

Butter, K.; Bomans, P. H.; Frederik, P. M.; Vroege, G. J. & Philipse, A. P. (2003). Direct observatioin of dipolar chains in ferrofluids in zero field using cryogenic electron microscopy, *J. Phys.: Conds. Matter.*, 15, 15, pp. S1451-S1470.

Camponeschi, E.; Florkowski, B.; Vance, R.; Garrett, G.; Garmestani, H. & Tannenbaum, R. (2006). Uniform directional alignment of single-walled carbon nanotubes in viscous polymer flow, *Langmuir*, 22, 4, pp. 1858-1862.

Camponeschi, E.; Vance, R.; Al-Haik, M.; Garmestani, H. & Tannenbaum, R. (2007). Properties of carbon nanotube-polymer composites aligned in a magnetic field, *Carbon*, 45, 10, pp. 2037-2046.

Camponeschi, E.; Walker, J.; Garmestani, H. & Tannenbaum R. (2008). Surfactant effects on the particle size of iron (III) oxides formed by sol-gel synthesis, *J. Non-Cryst. Solids*, 351, 34, pp. 4063-4069.

Chen, X. Q.; Saito, T.; Yamada, H. & Matsushige, K. (2001). Aligning single-wall carbon nanotubes with an alternating-current electric field, *Appl. Phys. Lett.*, 78, 23, pp. 3714-3716.

Correa-Duarte, M.A.; Grzelczak, M.; Salgueirino-Maceira, V. ; Giersig, M. ; Liz-Marzan, L. M.; Farle, M.; Sierazdki, K. & Diaz, R. (2005). Alignment of carbon nanotubes under low magnetic fields through attachment of magnetic nanoparticles, *J. Phys. Chem. B*, 109, 41, pp. 19060-19063.

deFaria, D. L. A.; Silva, S. V. & deOliveira, M. T. (1997). Raman microspectroscopy of some iron oxides and oxyhydroxides, *J. Raman Spectrosc.*, 28, 11, pp. 873-878.

Dou, S. X.; Yeoh, W. K.; Shcherbakova, O.; Wexler, D.; Li, Y.; Ren, S. M.; Munroe, P.; Chen, S . K.; Tan, S. K.; Glowacki, B. A. & MacManus-Driscoll, J. P. (2006). Alignment of carbon nanotube additives for improved performance of magnesium diboride superconductors. *Adv. Mater.*, 18, 6, pp. 785-788.

Fischer, J. E.; Zhou, W.; Vavro, J.; Llaguno, M. C.; Guthy, C. & Haggenmueller, R. (2003). Magnetically aligned single wall carbon nanotube films: Preferred orientation and anisotropic transport properties, *J. Appl. Phys.*, 93, 4, pp. 2157-2163.

Fujiwara, M.; Oki, E.; Hamada, M.; Tanimoto, Y.; Mukouda, I. & Shimomura, Y. (2001). Magnetic orientation and magnetic properties of a single carbon nanotube, *J. Phys. Chem. A*, 105, 18, pp. 4383-4386.

Garmestani, H.; Al-Haik, M. S.; Dahmen, K.; Tannenbaum, R.; Li, D.; Sablin, S. S. & Hussaini, M. Y. (2003). Polymer-mediated alignment of carbon nanotubes under high magnetic fields, *Adv. Mater.*, 15, 22, pp. 1918-1921.

Grzelczak, M.; Correa-Duarte, M. A. & Liz-Marzan, L. M. (2006). Carbon nanotubes encapsulated in wormlike hollow silica shells, *Small*, 2, 10, pp. 1174-1177.

Han, L.; Wu, W.; Kirk, F. L.; Luo, J.; Maye, M. M.; Kariuki, N. N.; Li, Y. H.; Wang, C. & Zhong, C. J. (2004). A direct route toward assembly of nanoparticle-carbon nanotube composite materials, *Langmuir*, 20, 14, pp. 6019-6025.

Hyeon, T.; Lee, S. S.; Park, J.; Chung, Y. & Bin, N. H. (2001). Synthesis of highly crystalline and monodisperse maghemite nanocrystallites without a size-selection process, *J. Am. Chem. Soc.*, 123, 51, pp. 12798-12801.

Jia, B.; Gao, L. & Sun, J. (2007). Self-assembly of magnetite beads along multiwalled carbon nanotubes via a simple hydrothermal process, *Carbon*, 45, 7, pp. 1476-1481.

Jorio, A.; Pimenta, M. A.; Souza, A. G.; Saito, R.; Dresselhaus, G.; & Dresselhaus, M. S. *New J. Phys.*, 5, 139.

Kim., I. T.; Nunnery, G.; Jacob, K.; Schwartz, J.; Liu, X. & Tannenbaum, R. (2010). Synthesis, characterization, and alignment of magnetic carbon nanotubes tethered with maghemite nanoparticles, *J. Phys. Chem. C*, 114, 15, pp. 6944-6951.

Kim, I. T.; Tannenbaum, A. & Tannenbaum, R. (2011). Anisotropic conductivity of magnetic carbon nanotubes embedded in epoxy matrices, *Carbon*, 49, 1, pp. 54-61.

Kimura, T.; Ago, H.; Tobita, M.; Ohshima, S.; Kyotani, M. & Yumura, M. (2002). Polymer composites of carbon nanotubes aligned by a magnetic field, *Adv. Mater.*, 14, 19, pp. 1380-1383.

Korneva, G.; Ye, H.; Gogotsi, Y.; Halverson, D.; Friedman, G.; Bradley, J. C. & Kornev, K. (2005). Carbon nanotubes loaded with magnetic particles, *Nano Lett.*, 5, 5, pp. 879-884.

Kuang, Q.; Li, S. F.; Xie, Z. X.; Lin, S. C.; Zhang, X. H.; Xie, S. Y.; Huang, R. B. & Zheng, L. S. (2006). Controllable fabrication of SnO_2-coated nanotubes by chemical vapor multiwalled carbon deposition, *Carbon*, 44, 7, pp. 1166-1172.

Lanticse, L. J.; Tanabe, Y.; Matsui, K.; Kaburagi, Y.; Suda, K.; Hoteida, M.; Endo, M. & Yasuda, E. (2006). Shear-induced preferential alignment of carbon nanotubes resulted in anisotropic electrical conductivity of polymer composites. *Carbon*, 44, 14, pp. 3078-3086.

Lourie, O.; Cox D. M. & Wagner H. D. (1998). Buckling and collapse of embedded carbon nanotubes, *Phys. Rev. Lett.*, 81, 8, pp. 1638-1641.

Lukic, B.; Seo J. W.; Bacsa R. R.; Delpeux, S.; Beguin, F.; Bister, G.; Fonseca, A.; Nagy, J. B.; Kis, A.; Jeney, S.; Kulik A. J. & Forro L. (2005). Catalytically grown carbon nanotubes of small diameter have a high Young's modulus, *Nano Lett.*, 5, 10, pp. 2074-2077.

Martin, C. A.; Sandler, J. K. W.; Windle, A. H.; Schwarz, M. K.; Bauhofer, W.; Schulte, K. & Shaffer, M. S. P. (2005). Electric field-induced aligned multi-wall carbon nanotube networks in epoxy composites, *Polymer*, 46, 3, pp. 877-886.

Matarredona, O.; Rhoads, H.; Li, Z. R.; Harwell, J. H.; Balzano, L. & Resasco, D. E. (2003). Dispersion of single-walled carbon nanotubes in aqueous solutions of the anionic surfactant NaDDBS, *J. Phys. Chem. B*, 107, 48, pp. 13357-13367.

Mei, Y.; Zhou, Z. J. & Luo, H. L. (1987). Electrical-resistivity of rf-sputtered iron-oxide thin-films, *J. Appl. Phys.*, 61, 8, pp. 4388-4389.

Millan, A.; Palacio, F.; Falqui, A.; Snoeck, E. ; Serin, V. ; Bhattacharjee, A. ; Ksenofontov, V. ; Gutlich, P. & Gilbert, I. (2007). Maghemite polymer nanocomposites with modulated magnetic properties, *Acta Mater.* 55, 6, pp. 2201-2209.

Nagahara, L. A.; Amlani, I.; Lewenstein, J. & Tsui, R. K. (2002). Directed placement of suspended carbon nanotubes for nanometer-scale assembly, *Appl. Phys. Lett.*, 80, 20, pp. 3826-3828.

Ounaies, Z.; Park, C.; Wise, K. E.; Siochi, E. J. & Harrison, J. S. (2003). Electrical properties of single wall carbon nanotube reinforced polyimide composites, *Compos. Sci. Technol.*, 63, 11, pp. 1637-1646.

Park, C.; Wilkinson, J.; Banda, S.; Ounaies, Z.; Wise, K. E.; Sauti, G.; Lillehei, P. T. & Harrison, J. S. (2006). Aligned single-wall carbon nanotube polymer composites using an electric field. *J. Poly. Sci. B: Poly. Phys.*, 44, 12, pp. 1751-1762.

Pascal, C.; Pascal, J. L.; Favier, F.; Moubtassim, M. L. E. & Payen, C. (1999). Electrochemical synthesis for the control of gamma-Fe_2O_3 nanoparticle size. Morphology, microstructure, and magnetic behavior, *Chem. Mater.*, 11, 1, pp. 141-147.

Peng, C. Q.; Thio, Y. S. & Gerhardt, R. A. (2008). Conductive paper fabricated by layer-by-layer assembly of polyelectrolytes and ITO nanoparticles, *Nanotechnology*, 19, 50, 505603.

Pileni, M. P. (2003). The role of soft colloidal templates in controlling the size and shape of inorganic nanocrystals, *Nature Mater.*, 2, 3, pp. 145-150.

Pu, H. T. & Jiang, F. J. (2005). Towards high sedimentation stability: magnetorheological fluids based on CNT/Fe_3O_4 nanocomposites, *Nanotechnology*, 16, 9, pp. 1486-1489.

Qu, L. T.; Dai, L.& Osawa, E. (2006). Shape/size-controlled syntheses of metal nanoparticles for site-selective modification of carbon nanotubes, *J. Am. Chem. Soc.*, 128, 16, pp. 5523-5532.

Rockenberger, J.; Scher, E. C. & Alivisatos, A. P. (1999). A new nonhydrolytic single-precursor approach to surfactant-capped nanocrystals of transition metal oxides, *J. Am. Chem. Soc.*, 121, 49, pp. 11595-11596.

Sincai, M.; Ganga, D.; Bica, D. & Vekas, L. (2001). The antitumor effect of locoregional magnetic cobalt ferrite in dog mammary adenocarcinoma, *J. Magn. Magn. Mater.*, 225, 1-2, pp. 235-240.

Sousa, M. H.; Rubim, J. C. ; Sobrinho, P. G. & Tourinho, F. A. (2001). Biocompatible magnetic fluid precursors based on aspartic and glutamic acid modified maghemite nanostructures, *J. Magn. Magn. Mater.*, 225, 1-2, pp. 67-72.

Steinert, B. W. & Dean, D. R. (2009). Magenetic field alignment and electrical properties of solution cast PET-carbon nanotube composite films, *Polymer*, 50, 3, pp. 898-904.

Sun, S. H.; Murray, C. B.; Weller, D.; Folks, L. & Moser, A. (2000). Monodisperse FePt nanoparticles and ferromagnetic FePt nanocrystal superlattices, *Science*, 287, 5460, pp. 1989-1992.

Sun, S. H.; Zeng, H.; Robinson, D. B.; Raoux, S.; Rice, P. M.; Wang, S. X. & Li, G. X. (2004). Monodisperse MFeO4 (M = Fe, Co, Mn) nanoparticles, *J. Am. Chem. Soc.*, 126, 1, pp. 273-279.

Sun, Z.; Liu, Z.; Wang, Y.; Han, B.; Du, J. & Zhang, J. (2005). Fabrication and characterization of magnetic carbon nanotube composites, *J. Mater. Chem.*, 15, 42, pp. 4497-4501.

Sun, Z. Y.; Yuan, H. Q.; Liu, Z. M.; Han, B. X. & Zhang, X. R. (2005). A highly efficient chemical sensor material for H_2S: alpha-Fe_2O_3 nanotubes fabricated using carbon nanotube templates, *Adv. Mater.*, 17, 24, pp. 2993-2997.

Treacy, M. M. J.; Ebbesen, T. W. & Gibsoj, J. M. (1996). Exceptionally high Young's modulus observed for individual carbon nanotubes, *Nature*, 381, 6584, pp. 678-680.

Yi, D. K.; Lee, S. S. & Ying, J. Y. (2006). Synthesis and application of magnetic nanocomposite catalysts, *Chem. Mater.*, 18, 10, pp. 2459-2461.

Youn, S.C.; Jung, D.; Ko, Y. K.; Jin, Y. W.; Kim, J. M. & Jung, H. (2009). Vertical alignment of carbon nanotubes using the magneto-evaporation method, *J. Am. Chem. Soc.*, 131, 2, pp. 742-748.

Yu, M. F.; Files, B. S.; Arepalli, S. & Ruoff, R. (2000). Tensile loading of ropes of single wall carbon nanotubes and their mechanical properties, *Phys. Rev. Lett.*, 84, 24, pp. 5552-5555.

Wan, J.; Cai, W.; Feng, J.; Meng, X. & Liu, E. (2007). In situ decoration of carbon nanotubes with nearly monodisperse magnetite nanoparticles in liquid polyols, *J. Mater. Chem.*, 17, 12, pp. 1188-1192.

Weber, M. & Kamal, M. R. (1997). Estimation of the volume resistivity of electrically conductive composites, *Polym. Compos.*, 18, 6, pp. 711-725.

White, W. B. & Deangeli, B. A. (1967). Interpretation of vibrational spectra of spinels, *Spectrochim. Acta, Part A*, A 23, 4, pp. 985-995.

Zhu, Y. F.; Ma, C.; Zhang, W.; Zhang, R. P.; Koratkar, N. & Liang, J. (2009). Alignment of multiwalled carbon nanotubes in bulk epoxy composites via electric field, *J. Appl. Phys.*, 105, 5, 054319.

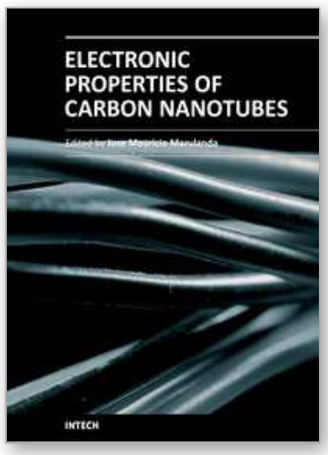

Electronic Properties of Carbon Nanotubes

Edited by Prof. Jose Mauricio Marulanda

ISBN 978-953-307-499-3
Hard cover, 680 pages
Publisher InTech
Published online 27, July, 2011
Published in print edition July, 2011

Carbon nanotubes (CNTs), discovered in 1991, have been a subject of intensive research for a wide range of applications. These one-dimensional (1D) graphene sheets rolled into a tubular form have been the target of many researchers around the world. This book concentrates on the semiconductor physics of carbon nanotubes, it brings unique insight into the phenomena encountered in the electronic structure when operating with carbon nanotubes. This book also presents to reader useful information on the fabrication and applications of these outstanding materials. The main objective of this book is to give in-depth understanding of the physics and electronic structure of carbon nanotubes. Readers of this book should have a strong background on physical electronics and semiconductor device physics. This book first discusses fabrication techniques followed by an analysis on the physical properties of carbon nanotubes, including density of states and electronic structures. Ultimately, the book pursues a significant amount of work in the industry applications of carbon nanotubes.

How to reference

In order to correctly reference this scholarly work, feel free to copy and paste the following:

Il T. Kim and Rina Tannenbaum (2011). Magnetic Carbon Nanotubes: Synthesis, Characterization, and Anisotropic Electrical Properties, Electronic Properties of Carbon Nanotubes, Prof. Jose Mauricio Marulanda (Ed.), ISBN: 978-953-307-499-3, InTech, Available from: http://www.intechopen.com/books/electronic-properties-of-carbon-nanotubes/magnetic-carbon-nanotubes-synthesis-characterization-and-anisotropic-electrical-properties

INTECH
open science | open minds

InTech Europe
University Campus STeP Ri
Slavka Krautzeka 83/A
51000 Rijeka, Croatia
Phone: +385 (51) 770 447
Fax: +385 (51) 686 166
www.intechopen.com

InTech China
Unit 405, Office Block, Hotel Equatorial Shanghai
No.65, Yan An Road (West), Shanghai, 200040, China
中国上海市延安西路65号上海国际贵都大饭店办公楼405单元
Phone: +86-21-62489820
Fax: +86-21-62489821

IntechOpen